JOURNAL OF MATERIALS SCIENCE 18 (1983) 1540–1547

The behaviour of 316L stainless steel in hydrogen

D. ELIEZER
Department of Materials Engineering, Ben-Gurion University of the Negev, Beer Sheva, Israel

Hydrogen embrittlement of 316L type austenitic stainless steel has been studied by charging thin tensile specimens (0.2 mm thick) with hydrogen through cathodic polarization. The effects of hydrogen on the phase transition and the relative role of the metallurgical variables is discussed. Room temperature cathodic charging of unstressed specimens produces intergranular and secondary transgranular cracks along crystallographic planes. Severe grain boundary spalling has been observed at longer times of charging indicating that high stresses were formed. The surface cracking that was observed during the ageing is consistent with the development of high tensile surface stresses. TEM studies of the fracture surfaces of both annealed and sensitized, fine and coarse grain size, have revealed high dislocation structure. Thin plates of hydrogen induced ϵ (h c p)-martensite was observed. These plates appear in a heavily faulted region. The evidence of faults within ϵ-plates indicates that the overlapping stacking fault mechanism for the austenite to ϵ transformation is in agreement with strain induced ϵ. The results of the tensile tests while undergoing cathodic charging show that the additional sensitization treatment and coarse-grained samples, lower the mechanical properties. The fracture surfaces of the sensitized steel contains regions of intergranular fracture where the micromechanism of the failure is microvoid nucleation and coalescence along grain boundaries. Finally, the microstructures are connected to various modes of cracking.

1. Introduction

Hydrogen embrittlement of austenitic stainless steels has been extensively studied during recent years [1–6]. Despite the large amount of previous work on the mechanism of hydrogen cracking, the relationship between hydrogen induced martensite and hydrogen related fracture has not been established.

The susceptibility of austenitic steels to hydrogen embrittlement has been attributed in part to α'-martensite [4, 6–9], co-planar dislocation motion [10, 11], impurity distribution at grain boundaries [8], surface effects [2, 12, 13] and the morphology of second phase precipitates [13–15]. Other metallurgical factors clearly play important roles in the degradation process, and it is unlikely that any single embrittlement model will be able to explain the relative roles of the important metallurgical variables [12–14]. One of the frequently discussed relationships is that between hydrogen induced martensite and hydrogen related fracture. Early work suggested that the formation of deformation induced martensite was essential for the embrittlement to be observed [7, 16]. This view arose because steels which partially transform to martensite upon straining, such as 304L, were found to be susceptible to hydrogen cracking whereas those with stable austenite phases, such as 310, were difficult to embrittle (stable and unstable are relative terms referring to the tendency toward martensitic transformation of the austenitic under normal conditions of processing and use of the steels). Odegard *et al.* [10] found that the susceptibility to hydrogen cracking in steels which did not transform to martensite upon deformation correlated very well with these parameters, and

0022–2461/84 $03.00 + .12

TABLE I Chemical composition of type 316L stainless steel (elements given in wt %)

Cr	Ni	Mn	Si	Co	Mo	Cu	N	P	C	S
17.65	11.10	1.80	0.50	0.35	2.08	0.21	0.061	0.03	0.026	0.009

that the fracture mode in hydrogen changed from ductile rupture to intergranular fracture as the embrittlement became more severe. Recently, it has been shown that the resistance to hydrogen embrittlement is improved by increasing the γ-phase stability [5, 17]. High voltage electron microscope (HVEM) observations of crack tips of type 304 specimens, which were severely embrittled by hydrogen pre-charging and then fractured in air have shown that the crack propagated mainly along the ϵ-martensite and partly in the region having a mixed structure of α' and ϵ-martensite phases [18]. In type 316L steel of intermediate γ stability it has been shown that the γ to ϵ phase transition occurs in front of the crack tip, where the crack propagation occurs mainly through the ϵ-phase while mixed area of α' within the ϵ-phase could be found ahead of the crack tip. It has been reported [19] that type 310 steel was embrittled by hydrogen and that the crack proceeded along the interface between austenite and the hydrogen induced ϵ-phase. Transformation from the f c c γ-phase to an expanded f c c phase γ^* and to the h c p ϵ-phase occurred during cathodic charging and has been reported by Narita *et al.* [6].

The occurrence of hydrogen embrittlement in austenitic stainless teels is substantial with ductility losses, and the appearance of nonductile fracture surfaces [1, 4, 5, 18–24]. The deleterious effect on mechanical properties caused by hydrogen charging has been found to depend strongly on metallurgical variables [5, 25–27]. Thus, for any given type of austenitic stainless steel, the susceptibility to hydrogen embrittlement will be influenced by austenitic instability resulting from cathodic charging, mechanical and thermal history, as well as changes in composition. It is necessary to develop a rather large data base in order to obtain better understanding of the behaviour of an austenitic stainless steel in a hydrogen environment. The present study will examine the effects of hydrogen on the phase transition, and the relative role of the metallurgical variables will be discussed.

2. Experimental procedure

Thin specimens, tensile tested while undergoing cathodic polarization were investigated as a function of both grain size and heat treatment. The steel was of commercial grade of compositions shown in Table I, and was received in the form of sheets 0.2 mm thick. Tensile specimens were prepared with their long axes parallel to the rolling direction according to [28]. Several austenitic grain sizes, ASTM 11, ASTM 8, ASTM 6 and ASTM 4, were obtained following various times at austenitizing temperatures. Some samples of each group were given a further heat treatment at 650° C for 24 h. This additional sensitization heat treatment should allow the precipitation of chromium carbides along grain boundaries. The samples were sealed in a charging cell and were tensile tested at room temperature at an extension rate of 0.005 cm min^{-1} while undergoing cathodic polarization. The hydrogen charging cell contained 1 N H_2SO_4 solution with 0.25 g l^{-1} of $NaAsO_2$, added as a hydrogen recombination poison. A platinum counter electrode and a current density of 50 mA cm^{-2} were used. Hydrogen ingress in the austenite matrix is performed by the electrolytic charging cell where hydrogen is liberated at the cathode surfaces and may diffuse into the sample interior. The impressed voltage driving the cell reaction provides a huge hydrogen fugacity and thus large amounts of hydrogen may be driven into the specimen.

For comparison purposes, specimens were tensile tested in air at room temperature. After failure the fractured surfaces were examined with a scanning electron microscope (SEM). Hydrogen effects on the martensitic transformation were studied using transmission electron microscopy (TEM). Characterization of the microstructural effects caused by the charging process was performed on pre-thinned specimens.

Specimens suitable for electron microscopy were prepared by electrolytic polishing at 65 V in a tenupol polishing cell using 30 cm^3 perchloric acid, 300 cm^3 methanol and 520 cm^3 butanol solution at −18° C. After a TEM examination to ensure that no deformation structure had been induced during the thinning process, the specimens were cathodically charged with hydrogen and were then investigated again by TM. The hydrogen charging was performed at room temperature in the absence of an external force in the charging

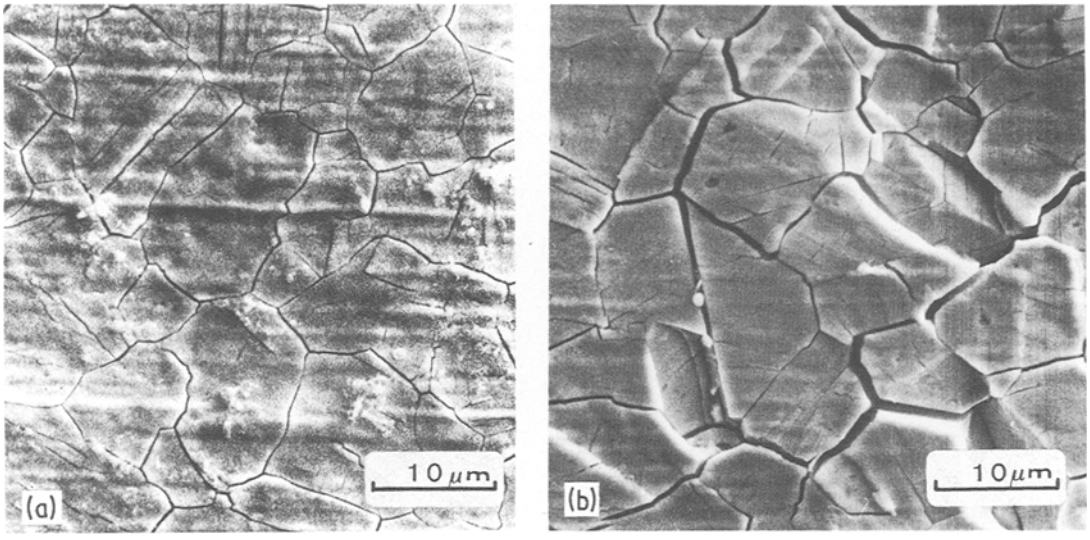

Figure 1 Scanning electron micrographs showing surface cracking produced in type 316L steel by cathodic charging of unstressed specimens at room temperature: (a) 24 h, and (b) 120 h.

conditions mentioned above. The charging time varied from a few minutes up to one hour. TEM analysis was carried out in a JEOL-200B electron microscope operating at 150 kV. The martensite formation was detected in connection with the susceptibility of the steel to hydrogen cracking. Implication of these findings on hydrogen embrittlement are discussed. An attempt is made to correlate the tensile properties of the hydrogen charged thin specimens with their mode of fracture.

3. Results and discussion

Previous work has established that surface cracking can be produced in austenitic stainless steels by cathodic charging in the absence of externally applied stresses [4, 29, 30]. This type of cracking was reproduced in the present work for 316L type steel. Figs. 1a and b depict intergranular and secondary transgranular cracks along crystallographic planes. Severe grain boundary spalling has been observed for longer times of charging (120 h), indicating that high stresses were formed. The depth of the cracks that propagate inside the material are of the order of 10 μm [31]. The relaxation of the internal stresses that are formed and the local increase in the shear stresses associated with preferential hydrogen outgassing through the grain boundaries plays an important role and is discussed elsewhere [32]. At the surface the hydrogen fugacity has been estimated to be at least 10^8 atm [33]. This would result in a surface concentration greater than about 12 at% H at equilibrium [34, 35]. The small lattice diffusivity of hydrogen in austenite ($D_H \sim 8 \times 10^{-16}$ m^2 sec^{-1} at 300 K [35]) coupled with its high fugacity is responsible for the attainment of the high surface concentrations during charging, and also the very high concentration gradients beneath the surface. Atrens *et al.* [36] have calculated the concen-

TABLE II Per cent reduction in tensile properties of specimens of type 316L stainless steel, tensile tested while undergoing cathodic polarization as compared to those of uncharged specimens

Heat treatment and grain size (ASTM number)	Yield strength	Ultimate tensile strength	Elongation (%)
Annealed ASTM 8	None	8	34
Sensitized ASTM 8	None	7	34
Annealed ASTM 6	None	5	38
Sensitized ASTM 6	None	12	42
Annealed ASTM 4	None	5	41
Sensitized ASTM 4	None	10	49

TABLE III Fracture modes in type 316L stainless steel, tensile tested while undergoing cathodic charging

Grain size (ASTM number)	Heat treatment	Fracture mode (% of surface)		
		Microvoid coalescence	Intergranular	Transgranular
8	Annealed	85	15	–
8	Sensitized	85	15	–
6	Annealed	85	–	15
6	Sensitized	50	45	5
4	Annealed	100	–	–
4	Sensitized	–	100	–

tration profiles resulting from hydrogen charging of austenite and have shown that immediately after the charging the hydrogen concentration falls by a factor of 10 within the first 5 μm of the surface. The surface cracking that was observed during the ageing is consistent with the development of high tensile surface stresses. An explanation of the reasons for the development of internal stresses as a result of cathodic charging and the correlation between the surface cracking and the internal stresses have been described elsewhere [31]. From a practical point of view, cracking could affect the mechanical behaviour when crack initiation on the surface is the determining step of the rupture process. The results given in Tables II and III demonstrate the influence of both grain size and heat treatment on the mechanical properties and the fracture mode of type 316L steel while undergoing cathodic polarization.

A significant feature of the results is that the sensitization treatment and coarse-grained samples, together, lower the mechanical properties of the steel. The yield and ultimate strengths were not much affected by sensitization, while significant changes in the ductility of the steel was observed. The sensitized coarse-grained specimens (ASTM 6) resulted in 42% reduction of elongation and 12% reduction of ultimate strength at fracture while the sensitized fine-grained specimens (ASTM 8) resulted in 34% reduction of elongation and 7% reduction of ultimate strength at fracture. By following the same conditions with coarser grain size (ASTM 4) the reduction of elongation at fracture was up to 49%. Another significance of the results is that the susceptibility of the fine-grained specimens is not changed by the additional heat treatment at 650° C for 24 h. The results show a slight reduction in ultimate strength for 34% reduction of elongation at fracture, whether the material was sensitized or not. Dimpled rupture was the main feature mode in both annealed and sensitized fine-grained 316L type steels (Fig. 2). Common features of this cracking were two narrow intergranular zones of about 10 μm on both fracture surface sides of the annealed and sensitized fine-grained specimens.

A predominantly intergranular fracture can be seen in sensitized 316L type steel by following the same conditions with coarser grain size – ASTM 4 (Fig. 3). A more detailed analysis of hydrogen induced cracking in annealed and sensitized fine- and coarse-grained 316L steel is given elsewhere [5]. Sensitization seems both to facilitate the penetration of hydrogen along grain boundaries into the steel and to introduce susceptibility to fracture along grain boundaries.

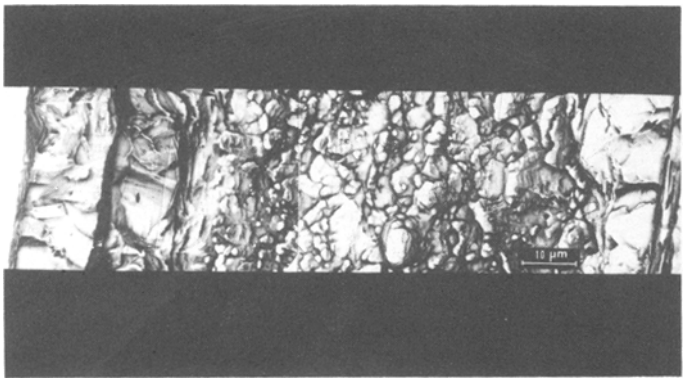

Figure 2 Scanning electron micrograph of fracture surface of the sensitized type 316L steel, grain size ASTM 8, tensile tested while undergoing cathodic charging.

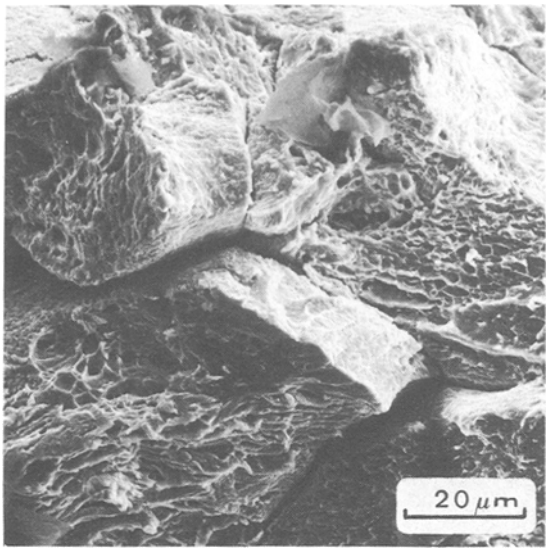

Figure 3 Scanning electron micrograph of the fracture surface of sensitized type 316L steel, grain size ASTM 4, tested while undergoing cathodic charging.

Fig. 4 shows a TEM micrograph of non-continuous grain boundary carbides ($Cr_{23}C_6$) in the sensitized steel. The sensitized 316L stainless steel failed intergranularly in hydrogen (Fig. 3) even though the carbides were not continuous along the grain boundaries, and that the surfaces of the solution annealed samples and samples given the additional sensitization heat treatment were quite similar. It has been suggested that the main reason for this was that chromium and carbon depletion at the boundaries allowed this region to transform to martensite upon deformation, thus providing an easy fracture path along the grain boundaries [37]. Our results show that the main fracture mode was completely intergranular (Table II and Fig. 3) only in the coarser grain size ASTM 4, while the intergranular fracture mode in per cent of surface was only 15% for the fine-grained samples (grain size ASTM 8) and 45% for grain size ASTM 6. The fracture mode in per cent of surface for 304L steel [5] was completely intergranular for grain size ASTM 6. These differences between the fracture mode of 304L and 316L types are probably due to the additional element molybdenum in type 316L. Molybdenum appears to increase the ease with which the steel passivates, thus more chromium depletion is required before sensitization will be detected.

It is suggested that the intergranular fracture is strongly related to both heat treatment and the grain size. Refined grain size improves resistance regardless of the failure mode. The origin of the effect [38] is probably not due to increased strengthening, but rather to an increasing number of trapping sites as the grain boundary area per unit volume increases. TEM studies of the fracture surface of both annealed and sensitized steel (fine and coarse grain size), tensile tested while under-

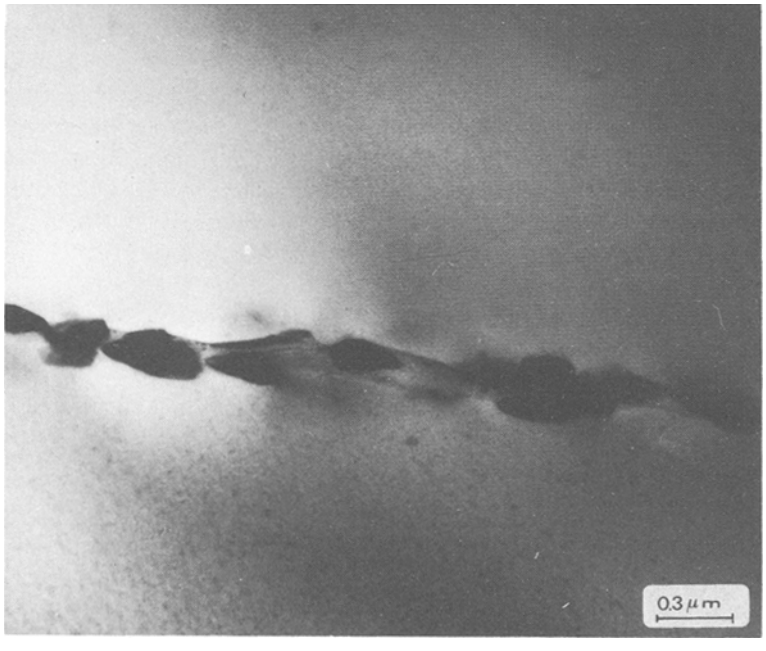

Figure 4 Transmission electron micrograph showing grain boundary carbides in the sensitized steel.

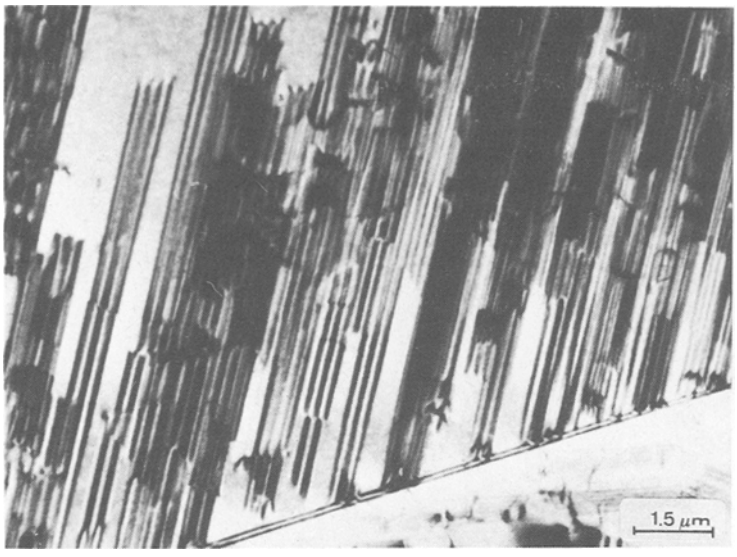

Figure 5 Transmission electron micrograph of the type 316L steel, which was cathodically charged with hydrogen shows a heavily faulted region caused by hydrogen charging.

going cathodic polarization have revealed high dislocation structure (Figs. 5 and 6). No evidence of the appearance of α'-martensite phase was found. However, recent investigation [15] on phase transitions at the crack tip in type 316L steel cathodically hydrogen charged in the absence of any externally applied stresses have revealed crack propagation through the mixed area of α'- and ϵ-martensite phase after hydrogen charging was found within the grains, in the thicker region of the specimen. The formation of ϵ-martensite by a process of overlapping stacking faults can be seen in TEM analysis [39] leads to the following orientation relationships between ϵ-martensite and the γ-matrix

$$(1\,1\,1)\gamma \parallel (0\,0\,0\,2)\epsilon$$

$$[0\,1\,\bar{1}]\gamma \parallel [1\,1\,\bar{2}\,0]\epsilon$$

This result demonstrates the appearance of hydrogen induced ϵ-phase in 316L steel (Fig. 7). It is consistent with other results previously reported for strain induced ϵ-phase in 310 and 304 steel [39, 41].

4. Conclusions

1. Room temperature cathodic charging of unstressed specimens produces intergranular and secondary transgranular cracks along crystllographic planes. Severe grain boundary spalling has been observed at longer times of charging indicating that high stresses were formed.

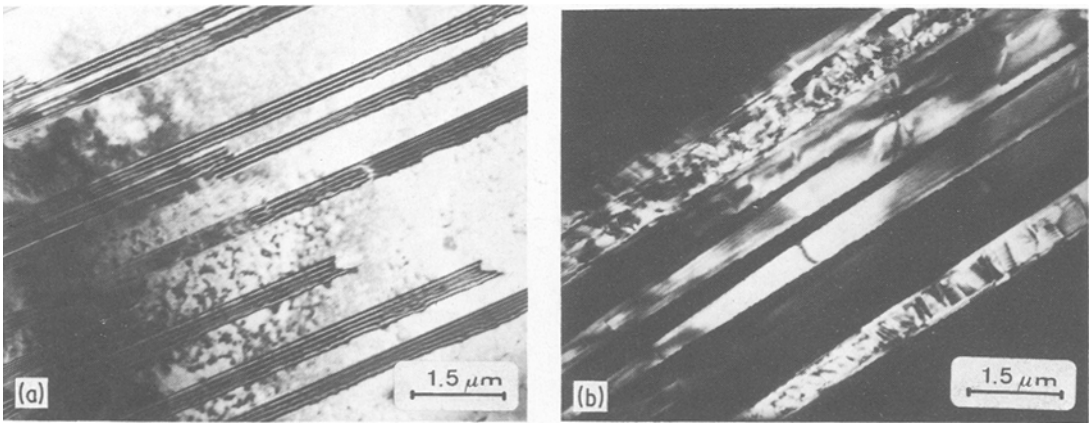

Figure 6 Transmission electron micrograph of the type 316L steel which was cathodically charged with hydrogen. The plates of ϵ-martensite can be seen (a) bright-field which shows the early stages of ϵ-martensite, and (b) dark-field, taken in the ϵ reflection.

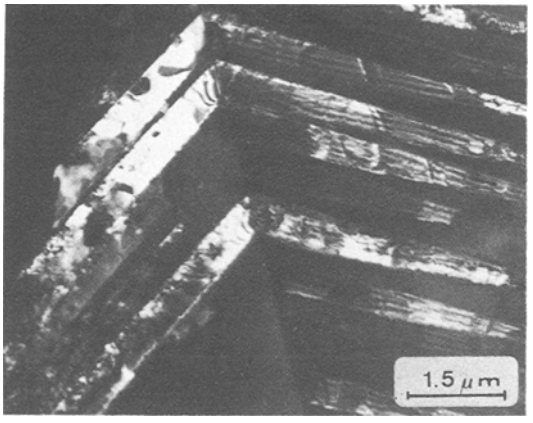

Figure 7 Transmission electron micrograph of type 316L steel which was cathodically charged with hydrogen. The grain boundary crack initiation sites are mainly meeting points of different families of ϵ-platelet on a grain boundary.

2. Refined grain size improves the resistance to hydrogen cracking regardless of the failure mode.

3. Sensitization seems both to facilitate the penetration of hydrogen along grain boundaries into the steel and to introduce susceptibility to fracture along grain boundaries.

4. The fracture surfaces of the sensitized steel contains regions of intergranular fracture where the micromechanism of the failure is microvoid nucleation and coalescence along grain boundaries.

5. Thin plates of hydrogen induced ϵ(hcp)-martensite was observed. These plates appear in a heavily faulted region. The evidence of faults within plates indicates that the overlapping stacking fault mechanism for the austenite to ϵ transformation is in agreement with the strain induced ϵ that was reported by others.

References

1. J. KOLTS, ASTM Publication ASTM STP 610 (ASTM, Pennsylvania, 1976) p. 336.
2. M. R. LOUTHAN Jr, "Hydrogen in Metals", edited by I. M. Bernstein and A. W. Thompson (ASM, Metals Park, Ohio, 1974) p. 54.
3. A. W. THOMPSON, "Environment-Sensitive Fracture of Engineering Materials", edited by A. Z. Foroulis (AIME, Warrendale, PA. 1979) p. 379.
4. D. ELIEZER, D. G. CHAKRPANI, C. J. ALTSTETTER and E. N. PUGH, *Met. Trans.* **10A** (1979) 935.
5. E. MINKOVITZ and D. ELIEZER, *J. Mater. Sci.* **17** (1982) 3165.
6. N. NARITA, C. J. ALTSTETTER and H. K. BIRNBAUM, *Met. Trans.* **13A** (1982) 1355.
7. R. B. BENSON, R. K. DANN and L. W. ROBERTS Jr, *Trans. TMS-AIME* **272** (1967) 2199.
8. C. L. BRIANT, *Metall. Trans.* **10A** (1979) 181.
9. E. MINKOVITZ and D. ELIEZER, *J. Mater. Sci. Lett.* **1** (1982) 192.
10. B. C. ODEGARD, J. A. BROOKS and A. J. WEST, "Effect of Hydrogen on Behavior of Materials", edited by A. W. Thompson and I. M. Bernstein (TMS, New York, NY, 1976) p. 116.
11. A. J. WEST and M. R. LOUTHAN Jr, *Metall. Trans.* **10A** (1979) 1675.
12. M. R. LOUTHAN Jr, G. R. CASKEY Jr, J. A. DONOVAN and D. E. RAWL Jr, *Mater. Sci. Eng.* **10** (1972) 357.
13. J. A. BROOKS and M. R. LOUTHAN Jr, *Metall. Trans.* **11A** (1980) 1981.
14. A. W. THOMPSON and J. A. BROOKS, *Metall. Trans.* **6A** (1975) 1931.
15. E. MINKOVITZ and D. ELIEZER, *Scripta Metall.* **16** (1982) 981.
16. R. M. VENNET and G. S. ANSELL, *Trans. ASM* **60** (1967) 242.
17. N. NARITA and H. K. BIRNBAUM, *Scripta Metall.* **14** (1980) 1355.
18. T. TAKAYAMA and M. TAKANO, *Corrosion* **38** (1982) 1.
19. A. INOUE, Y. HOSSOYA and T. NASUMOTO, *Trans. Iron Steel Inst., Jpn.* **19** (1979) 170.
20. M. L. HOLZWORTH, *Corrosion* **25** (1969) 107.
21. R. LAGNEBORG, *J. Iron Steel Inst.* **207** (1969) 363.
22. H. E. HANNINEN, *Int. Met. Rev.* **27** (1979) 85.
23. A. J. WEST Jr and M. R. LOUTHAN Jr, *Metall. Trans* **13A** (1982) 2049.
24. A. W. THOMPSON, "Environmental Degradation of Engineering Materials", edited by M. R. Louthan Jr and R. P. McNitt (Virginia Polytechnic Institute, Blacksburg, VA, 1977.
25. C. L. BRIANT, "Hydrogen Effects in Metals", edited by I. M. Bernstein and A. W. Thompson (TMS-AIME, Pennsylvania, 1980) p. 527.
26. H. HANNINEN, T. HAKKARAINEN and P. NENONEN, *ibid.* p. 575.
27. C. L. BRIANT and A. M. RITTER, *Scripta Metall.* **13** (1979) 177.
28. ASTM Standard Number E8.
29. M. RIGSBEE, *Metallography* **11** (1978) 493.
30. D. ELIEZER, "Hydrogen Effects in Metals", edited by I. M. Bernstein and A. W. Thompson (AIME, Warrendale, PA, 1981) p. 565.
31. P. ROZENAK, L. ZEVIN and D. ELIEZER, *J. Mater. Sci. Lett.* in press.
32. *Idem,* to be published.
33. A. KUMMICK and H. JOHNSON, *Metall. Trans.* **6A** (1975) 1087.
34. M. LOUTHAN and R. DERRICK, *Corros. Sci.* **15** (1975) 565.
35. P. STUDEBAKER, C. ALTSTETTER and W. CONLEY, "Hydrogen Effects in Metals", edited by I. M. Bernstein and A. W. Thompson (AIME Warrendale, PA, 1981) p. 169.
36. A. ATRENS, J. BELLINA, N. FIORE and R.

COYLE, "The Metal Science of Stainless Steels", edited by E. Collings and H. King (AIME, New York, NY, 1979) p. 54.
37. C. L. BRIANT, *Scripta Metall.* **12** (1978) 541.
38. I. M. BERNSTEIN and A. W. THOMPSON, "Alloy and Microstructural Design", edited by J. K. Tien and G. S. Ansell (Academic Press, New York, 1976) Chap. 9, p. 303.
39. E. MINKOVITZ, M. TALIANKER and D. ELIEZER, *J. Mater. Sci.* **16** (1981) 3506.
40. J. B. BROOKS, N. H. LORETTO and R. E. SMALLMAN, *Acta Metall.* **27** (1979) 1839.
41. R. LAGNEBORG, *ibid.* **12** (1964) 823.

Received 23 February
and accepted 18 March 1983